This is a 1D model of an active magnetic regenerative refrigerator (AMRR) that was developed in MATLAB. The model uses cycle inputs such as the fluid mass flow and magnetic field profiles, fluid and regenerator material properties, and regenerator geometry properties to generate the cyclical steady state temperature profile of the fluid and regenerator. Using the temperature profiles, the cooling load produced by the system and work input to the system are calculated. The development of the model is discussed in Progress Report #1. This model only considers the magnetic regenerator and does not model heat exchangers or other external hardware.

The model starts from an initial temperature profile for the regenerator and fluid and steps forward in time using implicit time steps until cyclical steady state is achieved. The user must define the number of time steps in each cycle and the number of nodes in the axial direction in the regenerator. Modeling parameters related to operating conditions, material properties, and geometry are determined by user-defined functions. New functions for each may be written to model systems that are not fully defined by the functions provided here.

Description of a One-Dimensional Numerical Model of an Active Magnetic Regenerator Refrigerator

1. Governing Equations

Figure 1 shows a schematic of an active magnetic regenerator modeled as a one dimensional (1D) system. The equipment that is external to the bed (e.g., the pumps, heat exchangers, and permanent magnets), are not explicitly modeled; however, their impact on the cycle is felt through an imposed time variation of the mass flow rate ($\dot{m}(t)$) and the variation of the magnetic field in time and space ($\mu_o H(x,t)$). The time variation of these quantities is related to the fluid-mechanical-magnetic processes associated with the cycle implementation. The interface between these imposed boundary conditions and the characteristics of these auxiliary pieces of equipment can be handled by system-level models that can interact with this component-level model.

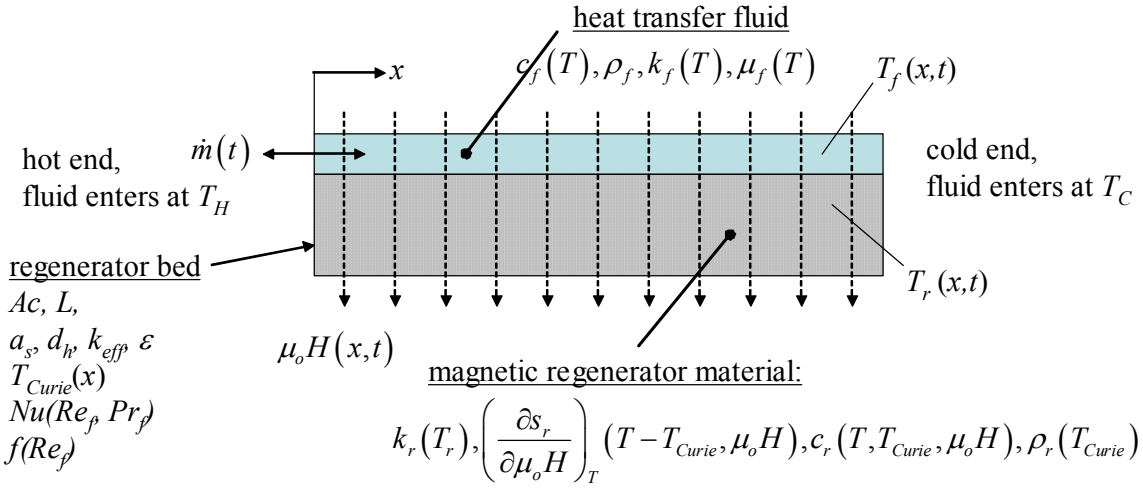

Figure 1. Conceptual drawing of a 1D AMR model showing the important parameters

A positive fluid mass flow rate indicates that flow is in the positive *x* direction, as indicated in Figure 1 and therefore enters the hot end of the regenerator bed; when it is negative it enters at the cold end. The fluid is assumed to be incompressible and therefore there can be no time variation in the mass of fluid that

is entrained in the bed. Continuity indicates that the mass flow rate must be spatially uniform within the bed so that the specification of the mass flow rate at the boundaries is sufficient to determine the mass flow rate throughout the bed. The flow entering the bed is assumed to have the temperature of the adjacent thermal reservoir, T_H or T_C depending on whether the flow rate is positive or negative, respectively. The required fluid properties include the density (ρ_f), specific heat capacity (c_f), viscosity (μ_f), and thermal conductivity (k_f). The specific heat capacity, viscosity, and thermal conductivity are assumed to be some function of temperature but not pressure. The density of the fluid is assumed to be unaffected by either temperature or pressure.

The fluid flows within a regenerator matrix composed of a magnetic material. The magnetic material may be layered; this layering may be represented simply as a spatial variation in the Curie temperature ($T_{Curie}(x)$) or, in more detail, as material properties that depend on the axial location within the bed. The partial derivative of the specific entropy of the material with respect to applied field at constant temperature is a function of the temperature of the material and of the applied magnetic field ($\frac{\partial s_r}{\partial \mu_o H}_T \left(T, \mu_o H\right)$). The specific heat capacity of the material at constant applied field of the material is assumed to be a function of the material's temperature and applied field and the conductivity is assumed to be a function of temperature ($c_{\mu_o H}\left(T, \mu_o H\right)$ and $k_r\left(T\right)$). The material is assumed to be incompressible and therefore has a constant density (ρ_r).

The geometry of the matrix must consist of many small passages that place the fluid in intimate thermal contact with the regenerator material. Regenerator geometries ranging from packed beds of spheres to screens to perforated plates may all be considered by this model by adjusting the thermal-fluid

correlations and the geometric parameters. In order to maintain this flexibility, the regenerator geometry is characterized by a hydraulic diameter (d_h), porosity (ε), and specific surface area (a_s). The Nusselt number of the matrix is assumed to be a function of the local Reynolds number and Prandtl number of the fluid ($Nu(Re_f, Pr_f)$). The friction factor is assumed to be a function of the local Reynolds number ($f(Re_f)$) and geometry. This friction correlation is sufficient for a steady or slowly modulating flows; however more sophisticated correlations requiring additional parameters may be required to characterize the oscillatory nature of the flow.

The matrix is characterized by an effective static thermal static conductivity (k_{eff}) that relates the actual, axial conduction heat transfer in the absence of fluid flow to the heat transfer through a comparable solid piece of material. Axial dispersion due to the eddy mixing of the fluid during fluid flow is treated as an augmented thermal conductivity in the fluid (k_{disp}). The values of these parameters depend on the particular geometry, materials, and flow conditions that are simulated. The overall size of the regenerator is specified according to its length (L) and total cross-sectional area (A_c).

The fluid and regenerator temperature variations over a steady-state cycle are the eventual output of the model ($T_f(x,t)$ and $T_r(x,t)$). These variations, coupled with the prescribed mass flow rate and material properties, allow the calculation of various cycle performance metrics such as the refrigeration load and the magnetic power requirement. These temperature variations are obtained by solving a set of coupled, partial differential equations in time and space. The governing differential equations are obtained from differential energy balances on the fluid and the matrix. Figure 2 illustrates a differential segment of the fluid with the various energy flows indicated.

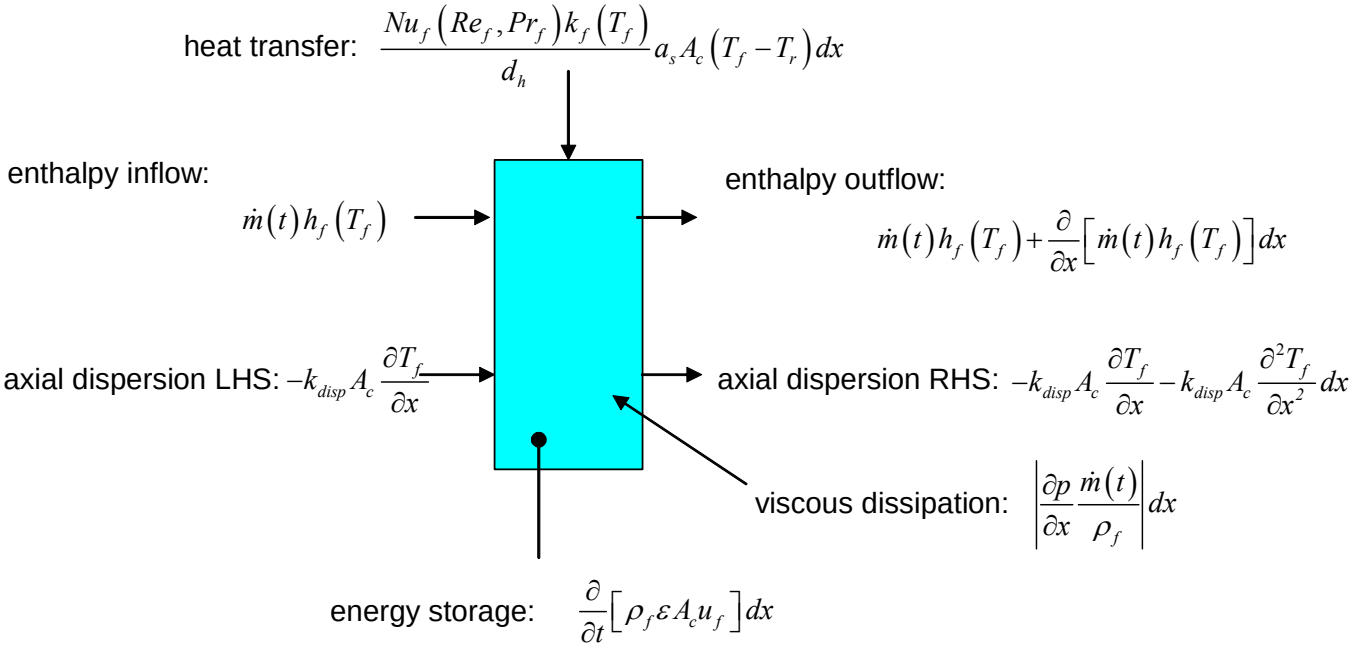

Figure 2. Differential segment of entrained fluid with energy terms indicated

After some simplification, the energy balance on the fluid suggested by Fig. 2 is:

$$k_{disp}A_c\frac{\partial^2 T_f}{\partial x^2}-\dot{m}\frac{\partial h_f}{\partial x}-\frac{Nu\,k_f}{d_h}a_s\,A_c\left(T_f-T_r\right)+\left|\frac{\partial p}{\partial x}\frac{\dot{m}}{\rho_f}\right|=\rho_f\,A_c\,\varepsilon\frac{\partial u_f}{\partial t} \qquad (1)$$

The first term in Eq. (1) represents conduction due to axial dispersion; the second term represents the change in the enthalpy carried by the fluid; the third term is the convective heat transfer between the fluid and the regenerator material; the fourth term represents viscous dissipation in the fluid, and the right side of the equation represents energy stored due to the heat capacity of the fluid entrained in the matrix. Note that axial conduction through the fluid is considered together with the axial conduction in the bed. Conduction in the fluid may be non-negligible due to its relatively high thermal conductivity. However, the axial conduction is applied to the matrix and modeled using the concept of an effective static bed conductivity. Note that the dispersive conductivity is much higher than the conductivity of the fluid whenever the fluid is flowing.

After expanding the derivatives in Eq. (1) under the assumption that material properties are independent of pressure and substituting the definition of the friction factor in terms of the pressure gradient, the energy balance becomes:

$$k_{disp} A_c \frac{\partial^2 T_f}{\partial x^2} - \dot{m} \frac{\partial h_f}{\partial T} \frac{\partial T_f}{\partial x} - \frac{Nu\, k_f}{d_h} a_s \; A_c \left(T_f - T_r \right) + \left| \frac{f_f \, \dot{m}^3}{2 \, \rho_f^2 \, A_c^2 \, d_h} \right| = \rho_f \; A_c \; \varepsilon \frac{\partial u_f}{\partial T} \frac{\partial T_f}{\partial t} \tag{2}$$

Assuming an incompressible fluid, Eq. (2) can be simplified to:

$$k_{disp} A_c \frac{\partial^2 T_f}{\partial x^2} - \dot{m}\, c_f \frac{\partial T_f}{\partial x} - \frac{Nu\, k_f}{d_h} a_s \; A_c \left(T_f - T_r \right) + \left| \frac{f_f \, \dot{m}^3}{2 \, \rho_f^2 \, A_c^2 \, d_h} \right| = \rho_f \; A_c \; \varepsilon \; c_f \frac{\partial T_f}{\partial t} \tag{3}$$

Figure 3 illustrates a differential segment of the regenerator material with the various energy flows indicated:

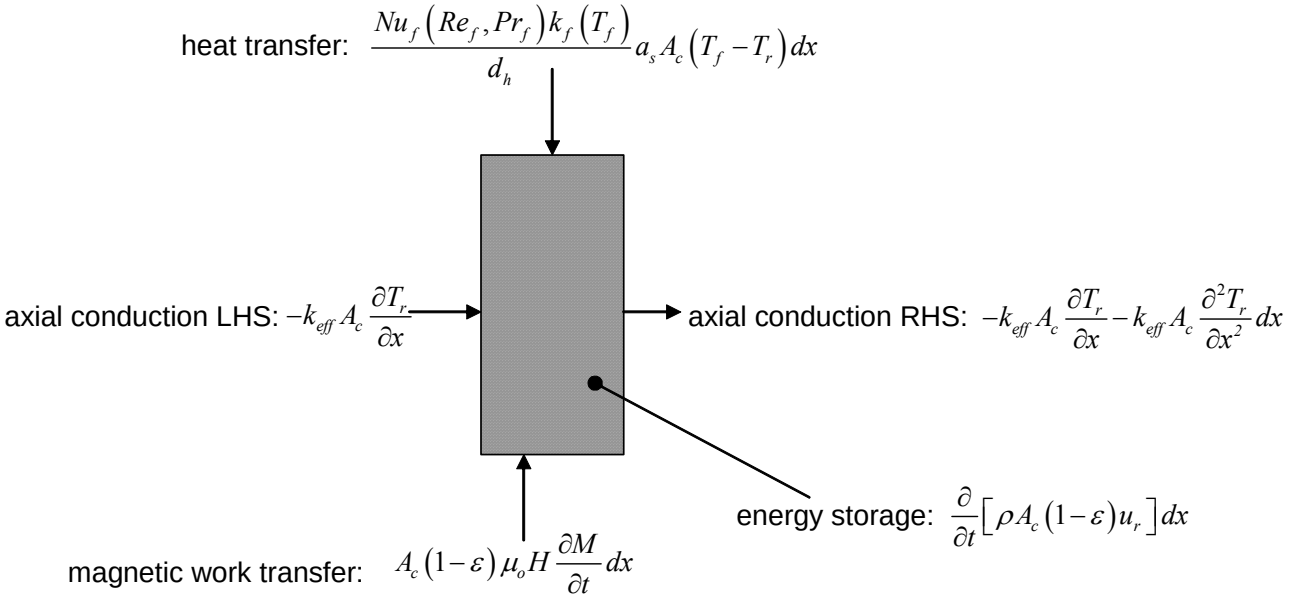

Figure 3. Differential segment of regenerator with energy terms indicated

The energy balance suggested by Figure 3 is:

$$\frac{Nu\ k_f}{d_h} a_s\ A_s \left(T_f - T_r\right) + A_c \left(1-\varepsilon\right) \mu_o H \frac{\partial M}{\partial t} + k_{eff} A_c \frac{\partial^2 T_r}{\partial x^2} = \rho_r\ A_c \left(1-\varepsilon\right) \frac{\partial u_r}{\partial t} \tag{4}$$

The magnetic work term is grouped with the internal energy to obtain:

$$\frac{Nu\ k_f}{d_h} a_s\ A_s \left(T_f - T_r\right) + k_{eff} A_c \frac{\partial^2 T_r}{\partial x^2} = A_c \left(1-\varepsilon\right) \rho_r \left(\frac{\partial u_r}{\partial t} - \mu_o H \frac{\partial \left(v_R M\right)}{\partial t} \right) \tag{5}$$

The right hand side of Equation (5) is the difference between a differential change in internal energy and a differential work transfer; this difference must be equal to a differential heat transfer, which is related to a change in entropy. Therefore, assuming the magnetization and demagnetization are reversible, Equation (5) may be rewritten according to:

$$\frac{Nu\ k_f}{d_h} a_s\ A_s \left(T_f - T_r\right) + k_{eff} A_c \frac{\partial^2 T_r}{\partial x^2} = A_c \left(1-\varepsilon\right) \rho_r\ T_r \frac{\partial s_r}{\partial t} \tag{6}$$

The change in regenerator entropy is divided into temperature and magnetic field driven components in order to yield the final, regenerator governing equation:

$$\frac{Nu\ k_f}{d_h} a_s\ A_s \left(T_f - T_r\right) + k_{eff} A_c \frac{\partial^2 T_r}{\partial x^2} = A_c \left(1-\varepsilon\right) \rho_r\ T_r \frac{\partial s_r}{\partial \mu_o H}_T \frac{\partial \mu_o H}{\partial t} + A_c \left(1-\varepsilon\right) \rho_r\ c_{\mu_o H} \frac{\partial T_r}{\partial t} \tag{7}$$

The fluid is assumed to enter the matrix at the temperature of the associated heat reservoir, providing the required spatial boundary conditions:

$$\begin{aligned} &\text{if } \dot{m}\left(t\right) \geq 0 \text{ then } T_f\left(x=0,t\right) = T_H \\ &\text{if } \dot{m}\left(t\right) < 0 \text{ then } T_f\left(x=L,t\right) = T_C \end{aligned} \tag{8}$$

The governing equations are integrated forward in time using a spatially implicit technique. A periodic steady state is achieved when the total energy change of the bed material (ΔU_r) and fluid entrained in the bed (ΔU_f) between the end of cycle *k* and the end of the previous cycle, *k-1*, normalized by the difference

between the maximum and minimum energy stored in the regenerator over the cycle is within a convergence tolerance (*tol*).

$$\frac{\Delta U_f + \Delta U_r}{U_{max} + U_{min}} < tol \qquad steady\ state \tag{9}$$

where the change in fluid energy is calculated by integrating the absolute value of energy change over the length of the bed.

$$\Delta U_f = \rho_f \varepsilon A_c \int_0^L \left| u_{f\,k} - u_{f\,k-1} \right| dx \tag{10}$$

and the change in regenerator energy is

$$\Delta U_r = \rho_r \left(1-\varepsilon\right) A_c \int_0^L \left| u_{r\,k} - u_{r\,k-1} \right| dx \tag{11}$$

and the energy stored in the fluid is

$$U_f = \rho_f \varepsilon A_c \int_0^L u_f dx \tag{12}$$

where T_{ref} is an arbitrarily chosen reference temperature. The energy of the regenerator material is calculated in same manner as the fluid energy. U_{max} is defined as the maximum sum of the fluid and regenerator energy at a given time step in the cycle and U_{min} is the minimum sum of fluid and regenerator energy. The numerical solution for the fluid and regenerator temperature is obtained over a spatial grid that extends from 0 to L as shown in Figure 4.

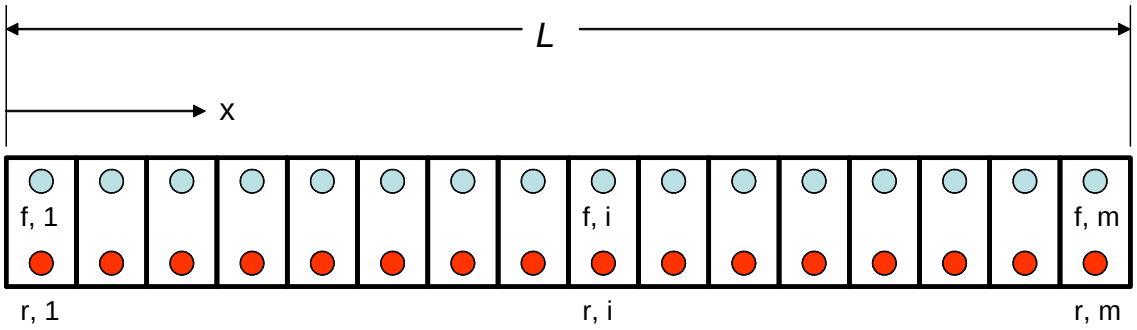

Figure 4. Numerical grid used for fluid and regenerator temperature solutions

The axial location of each fluid and regenerator temperature node (x_i) is given by:

$$x_i = \left(i - \frac{1}{2}\right)\frac{L}{m} \quad i=1..m \tag{13}$$

where i is the axial subscript and m is the total number of axial control volumes that are used. The cycle time is discretized by:

$$t_j = j\frac{\tau}{n} \quad j=0..n \tag{14}$$

where j is the temporal subscript and n is the total number of time steps that are used. Initial values for the temperatures at each spatial node ($T_{r\,i,1}$ and $T_{f\,i,1}$) can be assigned arbitrarily. One possibility is an assumed linear temperature profile, although other options are explored to speed convergence.

$$T_{r\,i,1} = T_H - \frac{x_i}{L}\left(T_H - T_C\right) \quad i=1..m \tag{15}$$

$$T_{f\,i,1} = T_H - \frac{x_i}{L}\left(T_H - T_C\right) \quad i=1..m \tag{16}$$

The changes in fluid and regenerator properties over a small time step are neglected so that the temperatures at time step $i+1$ are obtained using the discretized governing equations with constant

properties that are evaluated at time step *i*. The fluid energy balance is discretized and written for each control volume.

$$\frac{Nu_{i,j}\,k_{f\,i,j}}{d_h}\frac{a_s\,A_c L}{m}\left(T_{r\,i,j+1}-T_{f\,i,j+1}\right)+\dot{m}\left(t_j\right)c_{f\,i,j}\left(\frac{T_{f\,i,j+1}+T_{f\,i\text{-}1,j+1}}{2}-\frac{T_{f\,i+1,j+1}+T_{f\,i,j+1}}{2}\right)$$
$$+\left|\frac{f_{f\,i,j}\,\dot{m}\left(t_j\right)^3 L}{2\,\rho_f^2\,A_c^2\,d_h m}\right|+k_{disp\,i,j}A_c\frac{m}{L}\left(T_{f\,i\text{-}1,j+1}-T_{f\,i,j+1}\right)+k_{disp\,i,j}A_c\frac{m}{L}\left(T_{f\,i+1,j+1}-T_{f\,i,j+1}\right) \tag{17}$$
$$=\rho_f A_c\varepsilon c_f\frac{L\,n}{m\,\tau}\left(T_{f\,i,j+1}-T_{f\,i,j}\right)\qquad\qquad i=2..m-1$$

where $Nu_{i,j}$ is the Nusselt number based on the fluid temperature values in the node,

$$Nu_{i,j}=Nu\left(Re_{f\,i,j},Pr_{f\,i,j}\right) \tag{18}$$

Re_f is the Reynolds number for the fluid computed using the fluid temperature and the free flow velocity and $Pr_{f\,i,j}$ is the Prandtl number of the fluid:

$$Re_{f\,i,j}=\frac{d_h\left|\dot{m}\left(t_j\right)\right|}{A_c\,\mu_{f\,i,j}} \tag{19}$$

$$Pr_{f\,i,j}=\frac{c_{f\,i,j}\mu_{f\,i,j}}{k_{f\,i,j}} \tag{20}$$

The friction factor ($f_{f\,i,j}$) in Equation (14) is evaluated in terms of the local Reynold's number which depends upon the fluid temperatures within the node:

$$f_{f\,i,j}=f_f\left(Re_{f\,i,j}\right) \tag{21}$$

The boundary conditions for the fluid temperature governing equation are that fluid that enters at either edge of the regenerator has the temperature of the corresponding reservoir and that the edges of the bed are adiabatic with respect to dispersive heat transfer. At the boundaries of the regenerator bed, the energy

balance depends upon the fluid flow direction. The discretized fluid equations at the hot end of the regenerator bed are:

$$\begin{aligned}
&\textit{if } \dot{m}\left(t_j\right) \geq 0 \quad \textit{then} \\
&\frac{Nu_{1,j}\, k_{f\,1,j}}{d_h} \frac{a_s\, A_c L}{m} \left(T_{r\,1,j+1} - T_{f\,1,j+1}\right) + \dot{m}\left(t_j\right) c_{f\,1,j} \left(T_H - \frac{T_{f\;2,j+1} + T_{f\;1,j+1}}{2}\right) \\
&+ \left| \frac{f_{f\;1,j}\, \dot{m}\left(t_j\right)^3 L}{2\,\rho_f^2\, A_c^2\, d_h m} \right| + k_{disp\;1,j} A_c \frac{m}{L} \left(T_{f\;2,j+1} - T_{f\;1,j+1}\right) = \rho_f A_c \varepsilon\, c_f \frac{L\,n}{m\,\tau} \left(T_{f\;1,j+1} - T_{f\;1,j}\right) \quad \text{for } i = 1
\end{aligned} \tag{22a}$$

$$\begin{aligned}
&\textit{if } \dot{m}\left(t_j\right) < 0 \quad \textit{then} \\
&\frac{Nu_{1,j}\, k_{f\,1,j}}{d_h} \frac{a_s\, A_c L}{m} \left(T_{r\,1,j+1} - T_{f\,1,j+1}\right) - \dot{m}\left(t_j\right) c_{f\,1,j} \left(\frac{T_{f\;2,j+1} + T_{f\;1,j+1}}{2} - \left(\frac{3}{2} T_{f\;1,j+1} - \frac{1}{2} T_{f\;2,j+1}\right)\right) \\
&+ \left| \frac{f_{f\;1,j}\, \dot{m}\left(t_j\right)^3 L}{2\,\rho_f^2\, A_c^2\, d_h m} \right| + k_{disp\;1,j} A_c \frac{m}{L} \left(T_{f\;2,j+1} - T_{f\;1,j+1}\right) = \rho_f A_c \varepsilon\, c_f \frac{L\,n}{m\,\tau} \left(T_{f\;1,j+1} - T_{f\;1,j}\right) \quad \text{for } i = 1
\end{aligned} \tag{22b}$$

Note that, as shown in Figure 4, the temperature of each node is evaluated at the center of the node. Therefore, the temperature of the fluid exiting the hot end of the bed is approximated by extrapolating the temperatures in nodes 1 and 2. For node *m* (the cold end of the bed), the energy balances are:

$$\begin{aligned}
&\textit{if } \dot{m}\left(t_j\right) \geq 0 \quad \textit{then} \\
&\frac{Nu_{m,j}\, k_{f\,m,j}}{d_h} \frac{a_s\, A_c L}{m} \left(T_{r\,m,j+1} - T_{f\,m,j+1}\right) + \dot{m}\left(t_j\right) c_{f\,m,j} \left(\frac{T_{f\;m,j+1} + T_{f\;m\text{-}1,j+1}}{2} - \left(\frac{3}{2} T_{f\;m,j+1} - \frac{1}{2} T_{f\;m\text{-}1,j+1}\right)\right) \\
&+ \left| \frac{f_{f\;m,j}\, \dot{m}\left(t_j\right)^3 L}{2\,\rho_f^2\, A_c^2\, d_h m} \right| + k_{disp\;m,j} A_c \frac{m}{L} \left(T_{f\;m\text{-}1,j+1} - T_{f\;m,j+1}\right) = \rho_f A_c \varepsilon\, c_f \frac{Ln}{m\tau} \left(T_{f\;m,j+1} - T_{f\;m,j}\right) \quad \text{for } i{=}m
\end{aligned} \tag{23a}$$

$$\begin{aligned}
&\textit{if } \dot{m}\left(t_j\right) < 0 \quad \textit{then} \\
&\frac{Nu_{m,j}\, k_{f\,m,j}}{d_h} \frac{a_s\, A_c L}{m} \left(T_{r\,m,j+1} - T_{f\,m,j+1}\right) - \dot{m}\left(t_j\right) c_{f\,m,j} \left(T_C - \frac{T_{f\;m,j+1} + T_{f\;m\text{-}1,j+1}}{2}\right) \\
&+ \left| \frac{f_{f\;m,j}\, \dot{m}\left(t_j\right)^3 L}{2\,\rho_f^2\, A_c^2\, d_h m} \right| + k_{disp\;m,j} A_c \frac{m}{L} \left(T_{f\;m\text{-}1,j+1} - T_{f\;m,j+1}\right) = \rho_f A_c \varepsilon\, c_f \frac{L\,n}{m\,\tau} \left(T_{f\;m,j+1} - T_{f\;m,j}\right) \quad \text{for } i{=}m
\end{aligned} \tag{23b}$$

Collecting like terms in equations (17) leads to:

$$T_{f\,i,j+1}\left[\varepsilon\rho_f A_c\frac{L\,n}{m\,\tau}c_{f\,i,j}+Nu_{f\,i,j}\;k_{f\,i,j}\frac{a_s\;A_c L}{d_h m}+2k_{disp}A_c\frac{m}{L}\right]+T_{f\,i-1,j+1}\left[-\dot{m}\left(t_j\right)\frac{c_{f\,i,j}}{2}-k_{disp}A_c\frac{m}{L}\right]$$
$$+T_{f\,i+1,j+1}\left[\dot{m}\left(t_j\right)\frac{c_{f\,i,j}}{2}-k_{disp}A_c\frac{m}{L}\right]+T_{r\,i,j+1}\left[-\frac{Nu_{f\,i,j}\;k_{f\,i,j}}{d_h}a_s\;A_c\right]=T_{f\,i,j}\left[\varepsilon\rho_f A_c\frac{L\,n}{m\,\tau}c_{f\,i,j}\right] \qquad (24)$$
$$+\left|\frac{f^*_{i,j}\,\dot{m}\left(t_j\right)^3 L}{2\,\rho_f^2\,A_c^2\,d_h\,m}\right| \qquad i=2..m-1$$

Collecting terms for the hot end energy balance in equations (22a) and (22b) yields:

$$\textit{if}\;\;\dot{m}\left(t_j\right)\geq 0\quad\textit{then}$$
$$T_{f\,i,j+1}\left[\varepsilon\rho_f A_c\frac{L\,n}{m\,\tau}c_{f\,i,j}+\dot{m}\left(t_j\right)\frac{c_{f\,i,j}}{2}+Nu_{f\,i,j}\;k_{f\,i,j}\frac{a_s\;A_c L}{d_h\,m}+k_{disp}A_c\frac{m}{L}\right]+T_{f\,i+1,j+1}\left[\dot{m}\left(t_j\right)\frac{c_{f\,i,j}}{2}-k_{disp}A_c\frac{m}{L}\right]$$
$$+T_{r\,i,j+1}\left[-\frac{Nu_{f\,i,j}\;k_{f\,i,j}}{d_h}a_s\;A_c\right]=T_{f\,i,j}\left[\varepsilon\rho_f A_c\frac{L\,n}{m\,\tau}c_{f\,i,j}\right]+\left|\frac{f^*_{i,j}\,\dot{m}\left(t_j\right)^3 L}{2\,\rho_f^2\,A_c^2\,d_h\,m}\right|+\dot{m}\left(t_j\right)c_{f\,i,j}T_H$$
$$i=1$$

(25a)

$$\textit{if}\;\;\dot{m}\left(t_j\right)<0\quad\textit{then}$$
$$T_{f\,i,j+1}\left[\varepsilon\rho_f A_c\frac{L\,n}{m\,\tau}c_{f\,i,j}-\dot{m}\left(t_j\right)c_{f\,i,j}+Nu_{f\,i,j}\;k_{f\,i,j}\frac{a_s\;A_c L}{d_h m}+k_{disp}A_c\frac{m}{L}\right]+T_{f\,i+1,j+1}\left[\dot{m}\left(t_j\right)c_{f\,i,j}-k_{disp}A_c\frac{m}{L}\right]$$
$$+T_{r\,i,j+1}\left[-\frac{Nu_{f\,i,j}\;k_{f\,i,j}}{d_h}a_s\;A_c\right]=T_{f\,i,j}\left[\varepsilon\rho_f A_c\frac{L\,n}{m\,\tau}c_{f\,i,j}\right]+\left|\frac{f^*_{i,j}\,\dot{m}\left(t_j\right)^3 L}{2\,\rho_f^2\,A_c^2\,d_h m}\right|$$
$$i=1$$

(25b)

Collecting terms for the cold end fluid energy balance in equations (23a) and (23b) yields

$$
\begin{aligned}
&\textit{if } \dot{m}\left(t_j\right) \geq 0 \quad \textit{then} \\
&T_{f\,i,j+1}\left[\varepsilon \rho_f A_c \frac{L\,n}{m\,\tau} c_{f\,i,j} + \dot{m}\left(t_j\right) c_{f\,i,j} + Nu_{f\,i,j}\; k_{f\,i,j} \frac{a_s\; A_c L}{d_h m} + k_{disp} A_c \frac{m}{L}\right] \\
&+T_{f\,i-1,j+1}\left[-\dot{m}\left(t_j\right) c_{f\,i,j} - k_{disp} A_c \frac{m}{L}\right] + T_{r\,i,j+1}\left[-\frac{Nu_{f\,i,j}\; k_{f\,i,j}}{d_h} a_s\; A_c\right] \\
&= T_{f\,i,j}\left[\varepsilon \rho_f A_c \frac{L\,n}{m\,\tau} c_{f\,i,j}\right] + \left|\frac{f_{i,j}^{*}\, \dot{m}\left(t_j\right)^3 L}{2\,\rho_f^2\; A_c^2\; d_h\, m}\right| \qquad i = m
\end{aligned}
\tag{26a}
$$

$$
\begin{aligned}
&\textit{if } \dot{m}\left(t_j\right) < 0 \quad \textit{then} \\
&T_{f\,i,j+1}\left[\varepsilon \rho_f A_c \frac{L\,n}{m\,\tau} c_{f\,i,j} - \dot{m}\left(t_j\right) \frac{c_{f\,i,j}}{2} + Nu_{f\,i,j}\; k_{f\,i,j} \frac{a_s\; A_c L}{d_h m} + k_{disp} A_c \frac{m}{L}\right] \\
&+T_{f\,i-1,j+1}\left[-\dot{m}\left(t_j\right) \frac{c_{f\,i,j}}{2} - k_{disp} A_c \frac{m}{L}\right] + T_{r\,i,j+1}\left[-\frac{Nu_{f\,i,j}\; k_{f\,i,j}}{d_h} a_s\; A_c\right] \\
&= T_{f\,i,j}\left[\varepsilon \rho_f A_c \frac{L\,n}{m\,\tau} c_{f\,i,j}\right] - \dot{m}\left(t_j\right) c_{f\,i,j} T_C + \left|\frac{f_{i,j}^{*}\, \dot{m}\left(t_j\right)^3 L}{2\,\rho_f^2\; A_c^2\; d_h m}\right| \qquad i = m
\end{aligned}
\tag{26b}
$$

The regenerator energy balances are likewise discretized and written for each control volume:

$$
\begin{aligned}
&\frac{Nu_{f\,i,j}\; k_{f\,i,j}}{d_h} a_s\; A_s \frac{L}{m}\left(T_{r\,i,j+1} - T_{f\,i,j+1}\right) + A_c \frac{L}{m}\left(1-\varepsilon\right) \rho_r\; c_{\mu_o H\,i,j} \frac{\left(T_{r\,i,j+1} - T_{r\,i,j}\right) n}{\tau} \\
&+\frac{m\, k_{eff\;\,i,j}\; A_c}{L}\left[T_{r\,i,j+1} - T_{r\,i-1,j+1}\right] + \frac{m\, k_{eff\;\,i,j}\; A_c}{L}\left[T_{r\,i,j+1} - T_{r\,i+1,j+1}\right] = \\
&-A_c\left(1-\varepsilon\right) \rho_r T_{r\,i,j} \left(\frac{\partial s_r}{\partial \mu_o H}\right)_{i,j} \frac{\partial \mu_o H}{\partial t}\left(x_i, \frac{t_{j+1} + t_j}{2}\right) \qquad i = 2..m-1
\end{aligned}
\tag{27}
$$

Note that the 3rd and 4th terms in Eq. (27) represent conduction to the neighboring control volumes on the left- and right-hand sides, respectively. Collecting like terms leads to:

$$
\begin{aligned}
&T_{r\,i,j+1}\left[\frac{Nu_{i,j}\;k_{f\,i,j}}{d_h}a_s\;A_s+A_c\left(1-\varepsilon\right)\rho_r\;c_{\mu_o H\,i,j}\frac{Ln}{m\tau}+2\frac{m\,k_{eff\,i,j}\;A_c}{L}\right]\\
&+T_{r\,i-1,j+1}\left[-\frac{m\,k_{eff\,i,j}\;A_c}{L}\right]+T_{r\,i+1,j+1}\left[-\frac{m\,k_{eff\,i,j}\;A_c}{L}\right]+T_{f\,i,j+1}\left[-\frac{Nu_{i,j}\;k_{f\,i,j}}{d_p}a_s\;A_s\right]\\
&=-A_c\left(1-\varepsilon\right)\rho_r T_{r\,i,j}\left(\frac{\partial s_r}{\partial\mu_o H}\right)_{i,j}\frac{\partial\mu_o H}{\partial t}\left(x_i,\frac{t_{j+1}+t_j}{2}\right)+A_c\left(1-\varepsilon\right)\rho_r\;c_{\mu_o H\,i,j}T_{r\,i,j}\frac{Ln}{m\,\tau}\\
&i=1..m
\end{aligned}
\tag{28}
$$

The hot and cold ends of the regenerator are assumed adiabatic. Neglecting conduction at the edge of the bed, the energy balance at the hot end is:

$$
\begin{aligned}
&\frac{Nu_{f\,1,j}\;k_{f\,1,j}}{d_h}a_s\;A_s\frac{L}{m}\left(T_{r\,1,j+1}-T_{f\,1,j+1}\right)+A_c\frac{L}{m}\left(1-\varepsilon\right)\rho_r\;c_{\mu_o H\,1,j}\frac{\left(T_{r\,1,j+1}-T_{r\,1,j}\right)n}{\tau}\\
&+\frac{m\,k_{eff\,1,j}\;A_c}{L}\left[T_{r1,j+1}-T_{r\,2,j+1}\right]=-A_c\left(1-\varepsilon\right)\rho_r\,T_{r\,1,j}\left(\frac{\partial s_r}{\partial\mu_o H}\right)_{1,j}\frac{\partial\mu_o H}{\partial t}\left(x_{1i},\frac{t_{j+1}+t_j}{2}\right)
\end{aligned}
\tag{29}
$$

Neglecting conduction at the cold end, the energy balance at the cold end is:

$$
\begin{aligned}
&\frac{Nu_{f\,m,j}\;k_{f\,m,j}}{d_h}a_s\;A_s\frac{L}{m}\left(T_{r\,m,j+1}-T_{f\,m,j+1}\right)+A_c\frac{L}{m}\left(1-\varepsilon\right)\rho_r\;c_{\mu_o H\,m,j}\frac{\left(T_{r\,m,j+1}-T_{r\,m,j}\right)n}{\tau}\\
&+\frac{m\,k_{eff\,m,j}\;A_c}{L}\left[T_{r\,m,j+1}-T_{r\,m-1,j+1}\right]=-A_c\left(1-\varepsilon\right)\rho_r\,T_{r\,m,j}\left(\frac{\partial s_r}{\partial\mu_o H}\right)_{m,j}\frac{\partial\mu_o H}{\partial t}\left(x_{1i},\frac{t_{j+1}+t_j}{2}\right)
\end{aligned}
\tag{30}
$$

2. Numerical Solution Algorithm

Equations (24)-(26) and (28)-(30) form a system of linear equations in terms of each of the nodal regenerator and fluid temperatures that are shown in Figure 4 at one step forward in time. These equations are solved using a sparse matrix decomposition algorithm in order take a spatially implicit but temporally explicit step forward in time. This time step solution process is repeated in order to determine the fluid and regenerator temperatures at all spatial nodes and for each time step over an entire cycle. At

the end of each cycle, the change in energy in the regenerator and fluid is evaluated by performing the integration in equations (10) and (11) numerically and compared to the total energy in the fluid at the end of the cycle. When the absolute change in energy of the regenerator from cycle to cycle is within a specified tolerance, shown in Eq. (9), steady state has been achieved. This model is implemented in MATLAB.

The assumptions used to derive the numerical model were described as the model was derived in the previous section and are summarized below:

- the heat transfer fluid is incompressible; therefore the mass flow rate does not vary spatially within the matrix and the mass of fluid entrained in the matrix is constant,
- the bed geometry is uniform; no spatial gradients exist in the bed characteristics such as particle diameter, porosity, etc.,
- the fluid flow is one-dimensional; flow maldistribution effects are neglected, and
- the fluid flow is balanced,
- the magnetization and demagnetization processes are modeled as being internally reversible with no hysteresis or temperature gradients (note that this assumption is subsequently revisited and ultimately considered via a correction factor).

3. Verification of Model

There are no general analytical solutions to the regenerator equations presented above. However, in the limit of constant properties, no entrained fluid heat capacity and no axial conduction, a published solution for the thermal effectiveness (ε) of a conventional, passive regenerator (i.e., one with no magnetocaloric effect) subjected to a stepwise mass flow rate variation (with the shape shown in Figure 5) is available.

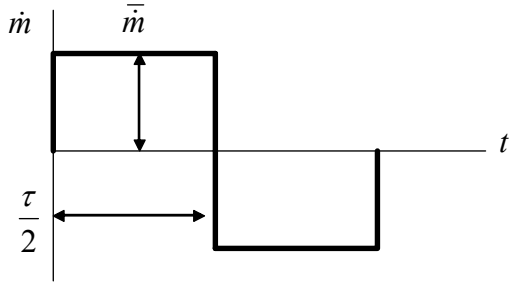

Figure 5. Mass flow rate variation for an idealized regenerator

According to Rohsenow et al. (1998), the thermal effectiveness (ε_t) for a regenerator with constant material properties is defined as:

$$\varepsilon_t \equiv \frac{c_f \int_0^{\tau/2} \dot{m}_f(t)\left(T_H - T_f\left(x=L,t\right)\right)dt}{\bar{\dot{m}}\, c_f \left(T_H - T_C\right)} \tag{31}$$

where $\bar{\dot{m}}$ is the magnitude of the mass flow rate function. The typical variables used to characterize this problem are the number of transfer units (*NTU*, sometimes also referred to as the reduced length of the regenerator) and the utilization ratio (*U*, the inverse of the matrix capacity rate ratio, Ackermann (1997)).

$$NTU \equiv \frac{Nu\, k_f\, a_s\, L\, A_c}{d_p\, \bar{\dot{m}}\, c_f} \tag{32}$$

$$U = \frac{\bar{\dot{m}}\, c_f\, \tau}{2\, A_c\, L\left(1-\varepsilon\right)\rho_r\, c_{\mu_o H}} \tag{33}$$

Dragutinovic and Baclic (1998) present tables for the ε_t as a function of *NTU* and *U* in this limit. The numerical model can be verified against these solutions by:

1. setting all fluid properties (c_f, k_f, ρ_f, and μ_f) equal to constants,
2. setting the partial derivative of entropy with respect to magnetic field equal to zero,

3. setting the remaining regenerator properties ($c_{\mu_o H}$ and ρ_r) equal to constants,
4. setting the effective thermal conductivity of the matrix (k_{eff}) and dispersion (k_{disp}) equal to zero,
5. setting the friction factor (f) equal to zero,
6. setting the specific surface area of the regenerator (a_s), particle diameter (d_p) and bed size (A_c and L) equal to constants,
7. applying the functional form of the mass flow rate shown in Figure 2.6 for a fixed cycle duration (τ),

$$\dot{m}(t) = sign\left(\frac{\tau}{2} - t\right)\bar{\dot{m}} \tag{34}$$

8. and setting the porosity (ε) to zero in order to specify zero entrained fluid heat capacity.

By varying the Nusselt number (Nu_f) and mass flow rate ($\bar{\dot{m}}$), it is possible to vary NTU and U. The numerical model was implemented under these conditions using a grid with 100 spatial control volumes (m = 100) and 3000 time steps (n = 3000). The results are illustrated in Figure 6. Notice the excellent agreement between the published and predicted results, verifying the accuracy of the numerical model in this limit. The results in Figure 6 are plotted in the region were effectiveness is greater than 0.9 in Figure 7.

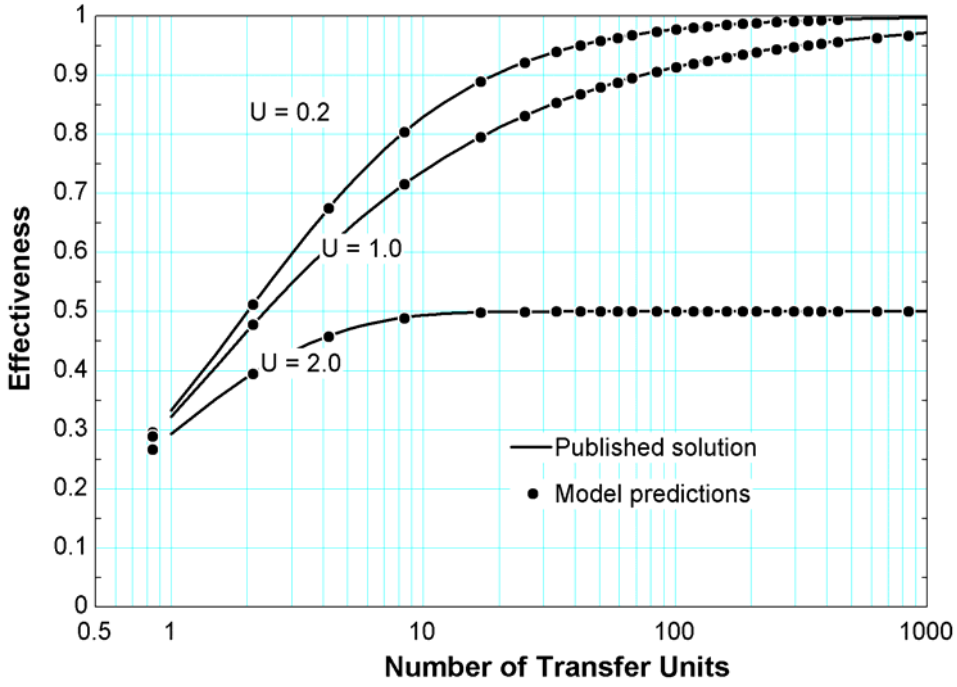

Figure 6. Numerical model predictions and published results for ε_t as a function of *NTU* and various values of *U* in the ideal regenerator limit

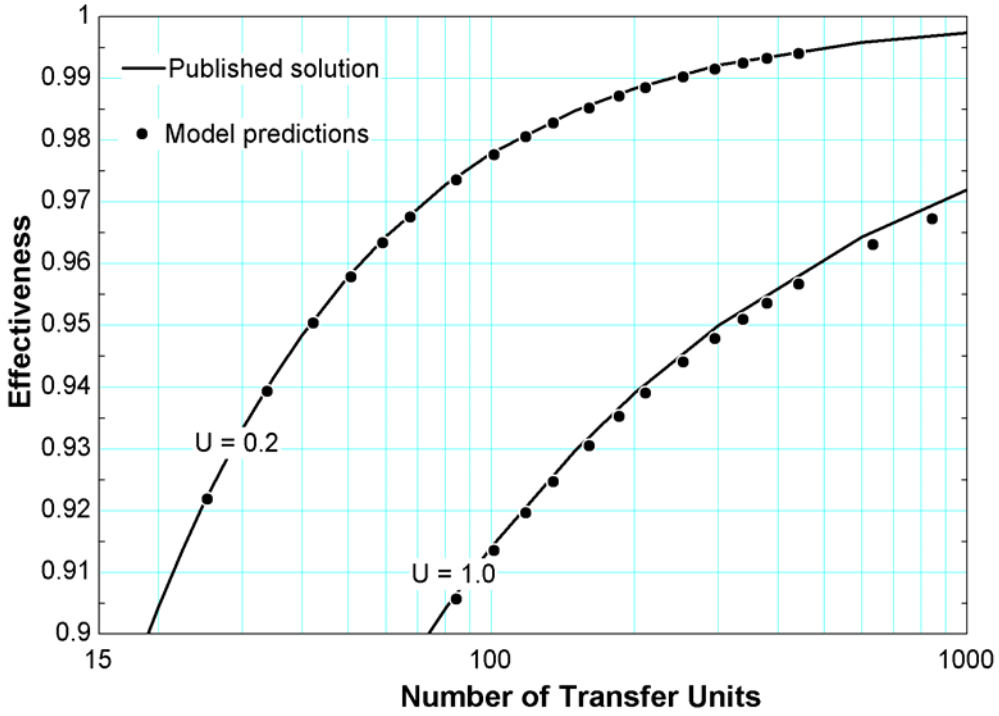

Figure 7. Numerical model predictions and published results from Figure 6 in the region $\varepsilon_t > 0.9$

Nomenclature

A_c	cross-sectional area (m^2)
a_s	specific surface area (m^2/m^3)
c	specific heat capacity (J/kg-K)
d_p	particle diameter (m)
f	friction factor
k	thermal conductivity (W/m-K)
k_{eff}	effective static thermal conductivity of regenerator and fluid (W/m-K)
k_{disp}	thermal conductivity of the fluid due to axial dispersion (W/m-K)
i	spatial subscript
j	temporal subscript
L	length (m)
m	number of axial control volumes used in numerical solution
$\dot{m}$	mass flow rate (kg/s)
M	magnetic intensity (A/m)
n	number of steps used in numerical solution
NTU	number of transfer units
Nu	Nusselt number
p	pressure (Pa)
Pr	Prandtl number
$\overline{\dot{q}}$	average heat transfer rate (W)
Re	Reynolds number
s	entropy (J/kg-K)
t	time (s)
tol	relaxation tolerance (K)
T	temperature (K)
T_{Curie}	Curie temperature (K)
u	internal energy (J/kg)
U	utilization factor
v	specific volume (m^3/kg)
x	axial position (m)

Greek

ε	porosity of matrix
ε_t	thermal effectiveness
μ	viscosity ($N\text{-}s/m^2$)
$\mu_o H$	applied field (Tesla)
ρ	density (kg/m^3)
τ	cycle duration (s)

Subscripts

C	cold or refrigeration temperature
f	fluid
H	hot or heat rejection temperature

r regenerator material

References

R. A. Ackermann, 1997, *Cryogenic Regenerative Heat Exchangers*, Plenum Press, New York.

G. D. Dragutinovic, and B. S. Baclic, 1998, *Operation of Counterflow Regenerators*, Computational Mechanics Inc., Billerica, MA.

W. M. Rohsenow, J. P. Hartnett and Y. I. Cho, 1998, *Handbook of Heat Transfer*, McGraw-Hill, New York, NY.